Temperature-dependent second harmonic generation process based on an MgO-doped periodically poled lithium niobate waveguide*

Shen Shi-Kui(沈世奎), Yang Ai-Ying(杨爱英)†, Zuo Lin(左 林), Cui Jian-Min(崔建民), and Sun Yu-Nan(孙雨南)

School of Opto-Electronics, Beijing Institute of Technology, Beijing 100081, *China*

(Received 8 March 2011; revised manuscript received 1 May 2011)

The temperature dependency of a 5-mol% MgO-doped periodically poled lithium niobate waveguide was investigated in this paper. We started with the temperature-dependent refractive index equation for the waveguide. Secondly, the temperature dependency of the second harmonic generation effect was experimentally researched under different temperatures and pump powers. The quasi-phase matched wavelengths, efficiency bandwidths and peak efficiencies of the waveguide were measured. The experimental results agreed with theoretical simulations, which are indispensable in the following all-optical sampling studies based on the cascaded second harmonic generation/difference-frequency generation process in the current device.

Keywords: periodically poled lithium niobate, second harmonic generation, quasi-phase matching, Sellmeier equation

PACS: 42.65.Ky, 42.65.Wi, 42.70.Mp **DOI:** 10.1088/1674-1056/20/10/104206

1. Introduction

Nonlinear processes based on second-order nonlinear interaction in periodically poled lithium niobate (PPLN) have been widely utilized due to their quasi-phase matching (QPM) condition; transparency of transmission data formats; bit rate independency; high conversion efficiency, lack of spontaneous emission noise; and other advantages. The important applications of these nonlinear processes include all-optical wavelength conversion,[1−4] all-optical sampling,[5−8] all-optical signal processing,[9] logic operation,[10,11] all-optical format conversion,[12] optical parametric oscillation,[13] and so on.

2. Temperature-dependent Sellmeier equation

In nonlinear interactions, two basic conditions must be satisfied, i.e. the energy conservation and the phase matching among the propagating waves. In PPLN, the QPM condition for extra-ordinary polarized waves is achieved by satisfying[14]

$$\Delta k = \frac{2\pi n_{\rm e}(\lambda_1, T)}{\lambda_1} - \frac{2\pi n_{\rm e}(\lambda_2, T)}{\lambda_2} - \frac{2\pi n_{\rm e}(\lambda_3, T)}{\lambda_3} - \frac{2\pi}{\Lambda(T)} = 0, \quad (1)$$

where Λ is the poling period and Δk is the phase mismatch. In the second harmonic generation (SHG) effect, the fundamental wave ($\lambda_{\rm p} = \lambda_2 = \lambda_3$) is converted to the second harmonic (SH) wave ($\lambda_{\rm sh} = \lambda_1 = 0.5\lambda_{\rm p}$). The dependence of the refractive index on wavelength and temperature must be accurately known. The Sellmeier equation provides information about the ordinary and extra-ordinary refractive indexes of nonlinear optical crystals. According to a modified Sellmeier equation, which has taken thermal effects into account, the temperature-dependent refractive index in undoped lithium niobate is given by[15]

$$n_{\rm e}^2(\lambda, T) = a_1 + b_1 f + \frac{a_2 + b_2 f}{\lambda^2 - (a_3 + b_3 f)^2} + \frac{a_4 + b_4 f}{\lambda^2 - a_5^2} - a_6\lambda^2. \quad (2)$$

All the parameters a_i and b_i are those given by Gayer for MgO-doped lithium niobate.[14] The b_i parameters

*Project supported by the National Natural Science Foundation of China (Grant Nos. 60777024 and 60978007).

†Corresponding author. E-mail: yangaiying@bit.edu.cn

© 2011 Chinese Physical Society and IOP Publishing Ltd

account for thermal effects, involving the temperature-dependent parameter f. For temperatures T expressed in Celsius degree (°C), f is given by

$$f = (T - 24.5\ ^\circ\mathrm{C})\,(T + 570.82\ ^\circ\mathrm{C})\,. \tag{3}$$

In addition, at elevated temperatures, the crystal also expands in the propagation direction and the actual poling period (Λ_T) of waveguide increases correspondingly. The thermal expansion coefficients of PPLN were described in Refs. [14] and [16], while thermal expansion of the crystal is not taken into account here.

3. Experimental setup of SHG

Figure 1 shows the experimental setup of the SHG process and a Z-cut 30-mm-long 5-mol%-MgO-doped PPLN waveguide (HC photonics) was used. A tunable continuous wave (CW) laser (Santec TSL-210) with a wavelength range of 1530 nm–1610 nm was used as a fundamental pump. EDFA was used to boost the pump and a variable optical attenuator was used to adjust the power. The polarization states of the pump light were adjusted by a polarization controller (PC) to obtain a high conversion efficiency because the waveguide was fabricated by using the anneal proton exchange (APE) technique, which only supports transverse-magnetic (TM) modes. The waveguide was mounted in an oven designed to offer optimum temperature control of the PPLN device. The temperature stability of the oven was about 0.1 °C. SH signals were measured by an optical spectrum analyser (OSA) (Anritsu, MS9710C) with a resolution of 0.1 nm.

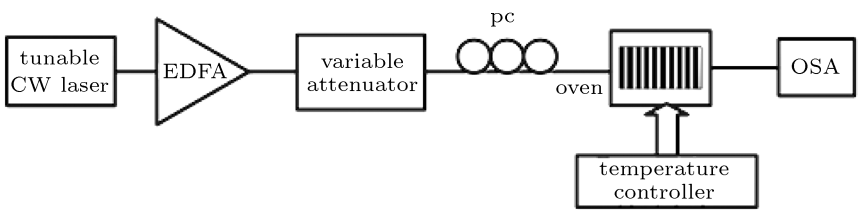


Fig. 1. Experimental setup for SHG measurement.

4. Results

For the lossless SHG process, the coupled-mode equation in the PPLN waveguide was derived based on a slowly varying envelope approximation. SH outputs of the waveguide with different pump wavelengths were measured at 62 °C. In Fig. 2, the SHG efficiency changes with the pump wavelength. The measured SHG efficiency (diamond-points) fits the theoretical result (solid line) with a nearly ideal sinc^2 shape curve. The deviation from the ideal sinc^2 shape may be caused by instability of the devices or environmental disturbance during measurement.

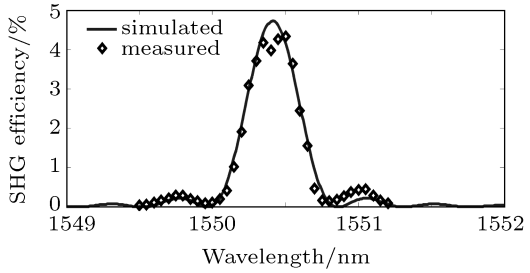


Fig. 2. Conversion efficiency versus input CW wavelength.

The actual poling period of the device was calculated as 19.2778 μm by formula (4) based on the temperature-dependent Sellmeier equation and the QPM condition, which agreed with the poling period of the PPLN waveguide of about 19.3 μm from the data sheet. The result verified the modified Sellmeier equation and parameters for 5-mol% MgO-doped PPLN in Ref. [14], which were used in solving the coupled mode equation of SHG process

$$\Lambda = 1/\left(\frac{n_\mathrm{e}\,(\lambda_\mathrm{sh}, T)}{\lambda_\mathrm{sh}} - \frac{2n_\mathrm{e}\,(\lambda_\mathrm{p}, T)}{\lambda_\mathrm{p}}\right), \tag{4}$$

SHG measurements in PPLN were also operated at different temperatures, i.e. 22 °C, 25 °C, 36 °C, 45 °C, 55 °C, and 70 °C. Using the tunable laser, SH signals at different temperatures were measured, with the wavelength step of about 0.05 nm. As shown in Fig. 3, different marks represent different temperatures, while the dashed lines are the corresponding thereotical simulation, with the wavelength step of 0.005 nm. Each curve has a nearly ideal sinc^2 shape, indicating that phase matching is maintained.

From Fig. 3, the QPM wavelengths and efficiency bandwidths at different temperatures are obtained.

Due to the temperature dependence of the refractive index of lithium niobate, the phase-matched wavelength varies with the temperature of the waveguide and the theoretical QPM wavelengths are calculated by formula (4). In Fig. 4, both the measured (diamond-points) and the simulated (dashed-line) QPM wavelengths increase with the heating of the device, and the maximal mismatch of the wavelengths is about 0.8 nm.

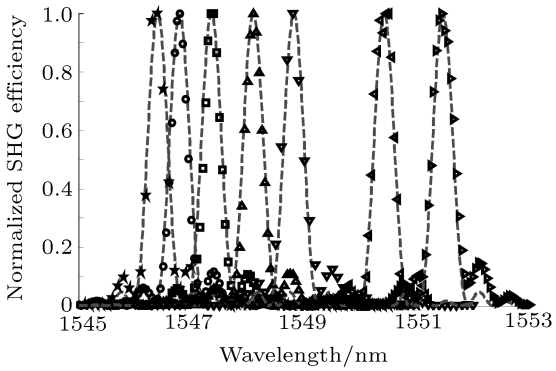


Fig. 3. Normalized efficiency at different temperatures.

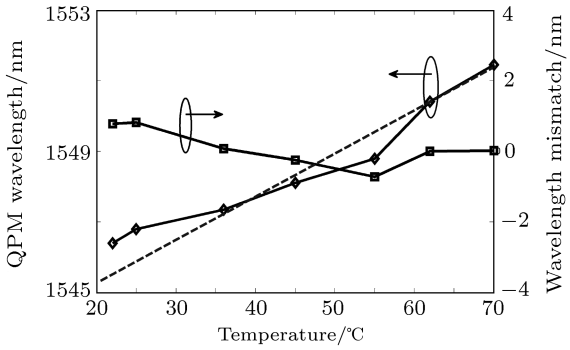


Fig. 4. QPM wavelength versus temperature.

The efficiency bandwidths were also calculated by best fit curves of the measured data in Fig. 3. The bandwidth curves are shown in Fig. 5, where diamonds represent measured results and circles the simulated results. Both the simulated and the measured bandwidths are about 0.4 nm as the temperature increases.

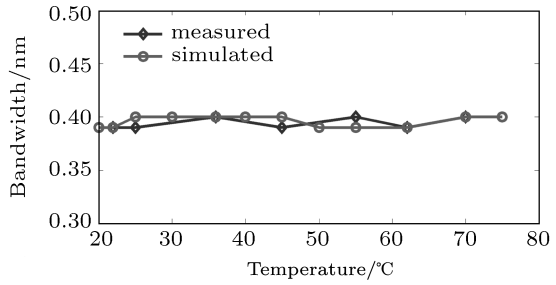


Fig. 5. Efficiency bandwidths versus temperatures.

Peak conversion efficiencies were measured at different pump powers, i.e. 7.3 dBm, 8.7 dBm, 9.1 dBm, 9.8 dBm, 13.2 dBm, 15.5 dBm, and 16.1 dBm. The efficiencies are shown in Fig. 6, where the diamonds represent the measured data and the dotted-dashed line represents the linear fitting of the measured data. There are other two lines in Fig. 6, the solid line represents the simulated curve with the transmission loss of the waveguide (0.35 dB·cm^{-1}@1550 nm, 0.7 dB·cm^{-1}@775 nm), while the dashed-line represents that without any loss. According to the results, both the simulated and the measured efficiencies increase with the fundamental pump power linearly. However, we found that the measured efficiencies are lower than the simulated results with transmission loss. The main reasons are as follows: (i) there was connection loss in the measurement; (ii) the pigtail of the waveguide was polarization maintaining fibre, so the SH signal has a larger loss when transmitting in multimode in pigtail; (iii) the pump light was amplified by EDFA, but the effective pump power was lower than the so-called pump power caused by the existence of amplified spontaneous emission (ASE) noise. It was noted that the slope of the measured curve was larger than that of the simulated curves. It was explained by the fact that the ASE noise decreased as the output of the EDFA increased. The results in Fig. 6 indicate that when the EDFA was used, the ASE noise should be eliminated by a bandpass filter.

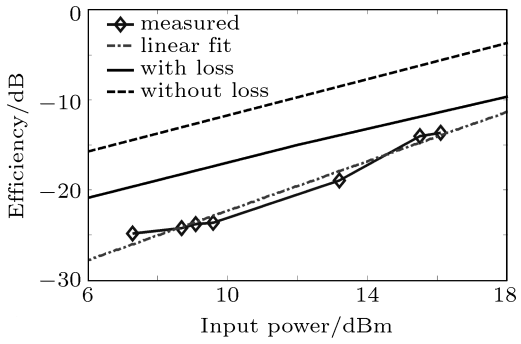


Fig. 6. Efficiency versus input pump power.

The power of the fundamental pump was set at 15.5 dBm and the efficiencies with loss and without transmission loss were calculated by theoretical simulation as the temperature varied from 20 °C to 90 °C. The efficiency curves are shown in Fig. 7, where the dashed-line represents the simulation without loss, the dot-dashed line is with loss and the diamonds represent the measured efficicencies at ten different temperatures from 26 °C to 87 °C. Both the simulated efficiencies decrease by only 0.2 dB as the temperature

increases by 70 °C, while the fluctuation of the measured efficiencies is about 0.4 dB within the temperature range of 61 °C. The gain variation of EDFA and instability during measurement would cause a larger fluctuation.

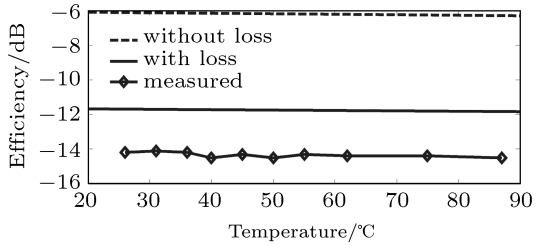


Fig. 7. Efficiency versus temperature at fixed pump power.

As the waveguide was mounted in temperature-controlled oven, the temperature tolerance of the device was measured. Pump wavelength was fixed at 1550.4 nm and the temperature was tuned from 62 °C at an interval 0.2 °C. Because the waveguide could only be heated up, only half of the curve was obtained. As shown in Fig. 8, the squares are experimental results and the solid line is the fitting. We found that the measured 3-dB temperature bandwidth is 1.6 °C. Under the assumption that the curve is symmetrical, the whole 3-dB bandwidth is about 3.2 °C while the simulated temperature bandwidth is 3.1 °C. A similar result was reported in Ref. [17], in which a bandwidth of 0.9 °C was obtained for the SHG process in bulk PPLN.

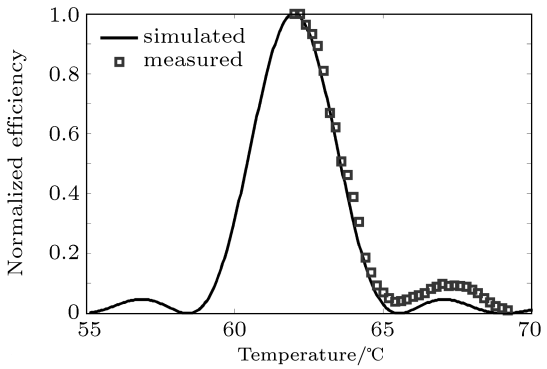


Fig. 8. Temperature tolerance of the waveguide.

5. Conclusion

The actual poling period of a PPLN waveguide was measured experimentally, which verified the modified temperature-dependent Sellmeier equation and the parameters for an MgO-doped PPLN device that were used in the theoretical simulation of the SHG process. The QPM wavelengths, bandwidth and peak efficiencies of the SHG process in the PPLN waveguide at different temperatures were measured, which are helpful for future all-optical sampling studies based on the cascaded second harmonic generation/difference-frequency generation process in the PPLN waveguide. The experimental results agree well with the theoretical simulation. The peak conversion efficiencies under different fundamental pump powers were studied.

References

[1] Wang Y, Fonseca C J, Xu C Q, Yang S Q, Ponomarev E A and Bao X Y 2006 *Appl. Opt.* **45** 5391

[2] Wang J, Sun J, Luo C and Sun Q 2006 *Appl. Phys.* B **83** 543

[3] Lee Y L, Yu B A, Jung C S, Noh Y C, Lee J M and Ko D K 2005 *Opt. Express* **13** 2988

[4] Hu H, Suche H, Ludwig R, Huettl B, Schmidt-Langhorst C, Nouroozi R, Sohler W and Schubert C 2009 *OSA/OFC/NFOEC*, San Diego, CA, USA OThS6

[5] Kawanishi S, Yamamoto T, Nakazawa and Fejer M M 2001 *Electron. Lett.* **37** 842

[6] Nogiwa S, Ohta H, Kawaguchi Y and Endo Y 1999 *Electron. Lett.* **35** 917

[7] Jungerman R L, Lee G, Buccafusca O, Kaneko Y, Itagaki N, Shioda R, Harada A, Nihei Y and Sucha G 2002 *IEEE Photon. Technol. Lett.* **14** 1148

[8] Yamada Nobuhide, Nogiwa Seiji and Ohta Hiroshi 2004 *IEEE Photon. Technol. Lett.* **16** 1125

[9] Langrock C, Kumar S, McGeehan J E, Willner A E and Fejer M M 2006 *J. Lightwave Technol.* **24** 7

[10] Kumar Garai S and Mukhopadhyay S 2010 *Optik* **121** 715

[11] Wang J, Sun J Q and Sun Q Z 2007 *Opt. Express* **27** 4

[12] Wang J, Sun J Q, Zhang X L, Huang D X and Fejer M M 2009 *IEEE J. Quantum Electron.* **45** 2

[13] Ding X, Zhang S M, Ma H M, Pang M, Yao J Q and Li Z 2008 *Chin. Phys.* B **17** 216

[14] Gayer O, Sacks Z, Galun E and Arie A 2008 *Appl. Phys.* B **91** 343

[15] Dieter J H, Fejer M M and Robert B L 1997 *IEEE J. Opt. Lett.* **22** 1553

[16] Paul O, Quosig A, Bauer T, Nittmann M, Bartschke J, Anstett G and L'Huillier J A 2007 *Appl. Phys.* B **86** 111

[17] Zhang J F, Chen Y P, Lu F and Chen X F 2008 *Opt. Express* **16** 6957